PCP
PLANT & CELL PHYSIOLOGY

Rapid Paper

Chaperone and Protease Functions of LON Protease 2 Modulate the Peroxisomal Transition and Degradation with Autophagy

Shino Goto-Yamada[1], Shoji Mano[1,2], Chihiro Nakamori[1], Maki Kondo[1], Ryuichi Yamawaki[3], Akira Kato[3,4] and Mikio Nishimura[1,2,*]

[1]Department of Cell Biology, National Institute for Basic Biology, Okazaki, 444-8585 Japan
[2]Department of Basic Biology, School of Life Science, The Graduate University for Advanced Studies, Okazaki, 444-8585 Japan
[3]Graduate School of Science & Technology, Niigata University, 8050, Ikarashi 2-no-cho, Nishi-ku, Niigata, 950-2181 Japan
[4]Department of Biology, Faculty of Science, Niigata University, 8050, Ikarashi 2-no-cho, Nishi-ku, Niigata, 950-2181 Japan
*Corresponding author: E-mail, mikosome@nibb.ac.jp; Fax, +81-564-53-7400.
(Received December 24, 2013; Accepted January 15, 2014)

Balancing repair and degradation is essential for maintaining organellar and cellular homeostasis. Peroxisomes are ubiquitous organelles in eukaryotic cells that play pivotal roles in cell survival. However, the quality control mechanism used to maintain peroxisomes is unclear. Here, we demonstrate that LON protease 2 (LON2), which is encoded by *ABERRANT PEROXISOME MORPHOLOGY 10* (*APEM10*), is responsible for the functional transition of peroxisomes with autophagy. The Arabidopsis *apem10* mutant displayed accelerated peroxisome degradation and a dramatically reduced number of peroxisomes. LON2 deficiency caused enhanced peroxisome degradation by autophagy, and peroxisomal proteins accumulated in the cytosol due to a decrease in the number of peroxisomes. We also show the proteolytic consequence of LON2 for the degradation of peroxisomal proteins, and we demonstrated that unnecessary proteins are eliminated by LON2- and autophagy-dependent degradation pathways during the functional transition of peroxisomes. LON2 plays dual roles as an ATP-dependent protease and a chaperone. We show that the chaperone domain of LON2 is essential for the suppression of autophagy, whereas its peptidase domain interferes with this chaperone function, indicating that intramolecular modulation between the proteolysis and chaperone functions of LON2 regulates degradation of peroxisomes by autophagy.

Keywords: *Arabidopsis thaliana* • Autophagy • Chaperone • Functional transition of peroxisomes • LON protease • Peroxisome.

Abbreviations: AAA+, ATPases associated with various cellular activities; *apem10*, *aberrant peroxisome morphology 10*; ATG2, autophagy-related 2; CAT, catalase; ConA, concanamycin A; ER, endoplasmic reticulum; GFP, green fluorescent protein; HPR, hydroxypyruvate reductase; ICL, isocitrate lyase; LACS6, long-chain acyl-CoA synthetase 6; LON2, LON protease 2; mRFP, monomeric red fluorescent protein; MS, malate synthase; pAPX, peroxisomal ascorbate peroxidase; *peup1*, *peroxisome unusual positioning 1*; PEX, PEROXIN; PMP38, peroxisomal membrane protein 38; PTS, peroxisome targeting signal; ROS, reactive oxygen species; WT, wild type.

Introduction

Peroxisomes are single membrane-bound organelles that are ubiquitous in eukaryotic cells. Peroxisomes have specialized functions depending on the organism or organ. Several different types of peroxisomes are present in higher plants, including glyoxysomes and leaf peroxisomes (Kamada et al. 2003). Peroxisomal functions are adapted in response to environmental and developmental cues. In post-germinative growth, glyoxysomes in etiolated cotyledons are transformed directly into leaf peroxisomes during the greening of cotyledons (Titus and Becker 1985, Nishimura et al. 1986). Glyoxysomes contain enzymes involved in β-oxidation and the glyoxylate cycle, which play a pivotal role in the conversion of lipids into sucrose, providing the energy needed for the post-germinative growth of seedlings. In green leaves, leaf peroxisomes are found widely in cells of photosynthetic organs and contain the enzymes that function in the glycolate pathway, which is active during photorespiration. During the functional transition of peroxisomes, glyoxysomal enzymes are specifically degraded, whereas leaf peroxisomal enzymes are newly synthesized and transported into peroxisomes as the greening of etiolated cotyledons proceeds (Titus and Becker 1985, Nishimura et al. 1986). This functional transition is also observed in senescing leaves, in which leaf peroxisomes are converted to glyoxysomes (Nishimura et al. 1993). Although it has been suggested that the functional transition of peroxisomes is controlled by gene expression,

Plant Cell Physiol. 55(3): 482–496 (2014) doi:10.1093/pcp/pcu017, available FREE online at www.pcp.oxfordjournals.org

protein translocation and protein degradation, the detailed mechanisms underlying these processes still need to be clarified (Nishimura et al. 1996, Kamada et al. 2003).

Whether the functional transition of peroxisomes proceeds in a linear and continuous fashion or a discontinuous and two-step fashion, called the 'one-population' and 'two-population' pathways, respectively, has been the subject of discussion since the 1970s (Beevers 1979). In the one-population hypothesis, glyoxysomes are directly transformed into leaf peroxisomes during the greening of cotyledons, and the insertion of newly synthesized leaf peroxisomal proteins occurs concomitantly with the degradation of glyoxysomal proteins (**Fig. 1A**). On the other hand, in the two-population hypothesis, glyoxysomes are eliminated and leaf peroxisomes are newly developed de novo (**Fig. 1B**). In the mid-1980s, using immunoelectron microscopic analysis, both glyoxysomal and leaf peroxisomal proteins were shown to co-exist in peroxisomes during the transition (Titus and Becker 1985, Nishimura et al. 1986), providing evidence that glyoxysomes are directly transformed into leaf peroxisomes as proposed by the one-population hypothesis. However, the detailed molecular mechanisms underlying this process remain to be elucidated.

The mechanism used to remove unnecessary and toxic cellular components in the maintenance of homeostasis is found among various organelles and cellular processes (Leidhold and Voos 2007, Buchberger et al. 2010, Youle and van der Bliek 2012). Since peroxisomes produce hydrogen peroxide (H_2O_2) in the course of their metabolism and since H_2O_2 can be the source of the most highly reactive and toxic form of reactive oxygen species (ROS), peroxisomal proteins must be damaged by this process. Therefore, a quality control system that removes abnormal and toxic proteins is important for maintaining the optimal performance of peroxisomes. In Arabidopsis peroxisomes, five proteases, including LON protease 2 (LON2), Tysnd1 homolog DEG15 and M16 protease, are reported to represent a putative protease (Lingard and Bartel 2009), and six putative chaperone-related proteins have been identified (Reumann et al. 2009). However, the roles of these proteases and chaperones in the quality control of peroxisomes are still unknown. In addition, peroxisomes contain ubiquitin-conjugating enzyme [PEROXIN 4 (PEX4)], ubiquitin protein ligases (PEX2, PEX10 and PEX12) and AAA ATPases (PEX1 and PEX6), which are reported to play roles in the protein export system (Collins et al. 2000). These enzymes are known as analogs of components of the endoplasmic reticulum (ER)-associated protein degradation system (ERAD) (Schluter et al. 2006, Buchberger et al. 2010). Mutants defective in PEX4 function show a delay in peroxisomal matrix protein degradation during germinative growth, suggesting that this export system is involved in the translocation of unnecessary proteins for cytosolic proteasomal degradation (Lingard et al. 2009). Recently, peroxisome degradation by autophagy was identified as an alternative mechanism for quality control of peroxisomes (Iwata et al. 2006, Sakai et al. 2006). Autophagy, which removes unnecessary or dysfunctional cellular components through the

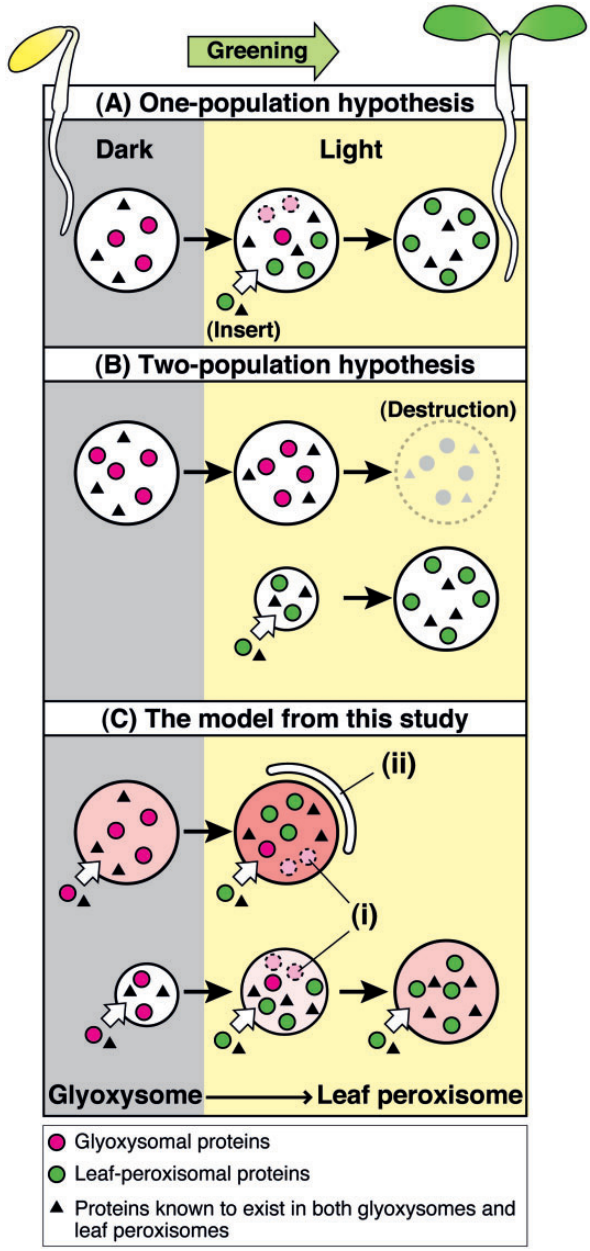

Fig. 1 Two hypothetical mechanisms proposed for the functional transition of glyoxysomes to leaf peroxisomes and a new model based on the results of this study. In the 'one-population' (A) and 'two-population' (B) hypotheses, peroxisomal transformation proceeds in a continuous and discontinuous fashion, respectively. In the new model (C), glyoxysomal proteins (magenta circles) are synthesized and transported to peroxisomes in etiolated cotyledons. After light is received, the cotyledons become green, and the glyoxysomes are transformed into leaf peroxisomes, in which leaf peroxisomal proteins (green circles) are transported and glyoxysomal proteins are degraded by LON2 (i). In parallel, excess or oxidized peroxisomes are degraded by autophagy (ii). LON2 chaperone function suppresses autophagy, and some glyoxysomes are successfully transformed into leaf peroxisomes during these processes. Triangles indicate proteins known to exist in both glyoxysomes and leaf peroxisomes. The intensity of the red coloring in the peroxisomes in (C) represents the level of hydrogen peroxide.

actions of the vacuole/lysosome, functions as an intracellular degradation process. In yeast cells, excess peroxisomes are selectively degraded by autophagy, which is known as pexophagy (Sakai et al. 2006). Catalase (CAT) is inactivated by H_2O_2 during the detoxification of H_2O_2, which leads to the formation of protein aggregates inside peroxisomes. Recently, we demonstrated that peroxisomes are gradually oxidized by ROS as inactivation of CAT proceeds, and that these oxidized peroxisomes are selectively degraded by autophagy in plants (Shibata et al. 2013). Although it is becoming clear that various pathways are involved in peroxisome quality control in plants, the detailed mechanisms of each pathway remain to be elucidated.

Previously, we screened chemically mutagenized transgenic Arabidopsis plants that express peroxisome-targeted green fluorescent protein (GFP) to identify mutants defective in peroxisome biogenesis, morphology and function (Mano et al. 2002). We isolated several *aberrant peroxisome morphology* (*apem*; previously referred to as *apm*) mutants that had different GFP fluorescence patterns from those of the parental plants (Mano et al. 2004, Mano et al. 2006, Goto et al. 2011, Mano et al. 2011). In this study, we report the identification and characterization of APEM10 as the peroxisomal protease LON2. The loss of function of LON2 leads to accelerated autophagy, accumulation of electron-dense inclusions in the peroxisome matrix and a delay in the elimination of glyoxysomal enzymes during post-germinative growth. We propose that LON2 is involved in the peroxisomal functional transition and basal quality control of peroxisomes. In these processes, LON2 modulates autophagy via its chaperone activity.

Results

The phenotype of the *apem10* mutant

Peroxisomes have specialized functions depending on the organism or organ, and their functions adapt to environmental and developmental cues in plant cells (Beevers 1979). To better understand this process, we previously isolated a number of peroxisome mutants, the *apem* mutants, based on their different pattern of GFP fluorescence from that of the parent plant expressing the peroxisome marker GFP–PTS1 (Mano et al. 2004, Mano et al. 2006, Goto et al. 2011, Mano et al. 2011), in which GFP fluorescence is observed as punctate peroxisomal signals in most cells (**Fig. 2A**). One *apem* mutant, *apem10*, showed a decrease of punctate GFP signals and accumulation of GFP fluorescence in the cytosol. These phenotypes were not observed in young tissues such as emerging new leaves and root tips, but were observed in mature tissues including fully expanded leaves, the upper parts of roots, and root caps (**Fig. 2A**). In addition, 4- to 5-week-old *apem10* mutants contained enlarged peroxisomes, whose maximum diameter was 20 μm (**Fig. 2B, C**). The appearance of the *apem10* phenotype depended on the growth conditions; nitrogen depletion caused severe cytosolic GFP accumulation even in emerging new leaves, and high CO_2 conditions (1% CO_2), in which the photorespiratory pathway did not function, suppressed the enlargement of peroxisomes in *apem10* (**Supplementary Fig. S1**). Enlarged peroxisomes frequently contained a region not visualized with GFP (**Fig. 2C**). Electron microscopic observation showed that enlarged peroxisomes contained electron-dense regions along the inner peroxisomal periphery (**Fig. 2D**), and immunogold labeling with antibodies against GFP revealed that gold particles rarely localized to electron-dense regions, although they normally localized to non-electron-dense regions of peroxisomes (**Fig. 2E**), which is in good agreement with the GFP fluorescence results. Oxidized peroxisomes accumulate inactivated CAT, a peroxisomal enzyme, and such aggregates are observed as electron-dense regions (Shibata et al. 2013). Gold particles conjugated with antibodies against CAT localized to electron-dense regions, indicating that abnormal CAT accumulates in *apem10* (**Fig. 2E**). These results suggest that *APEM10* plays an important role in the number and morphology of peroxisomes.

The *APEM10* gene encodes LON2

Map-based cloning identified the *APEM10* locus between the MPL12 and K14A3 BAC (bacterial artificial chromosome) clones on chromosome 5, which contains 106 predicted genes. We found a single nucleotide substitution of C to T in the fourth exon of At5g47040, which is annotated as *Lon protease 2* (*LON2*). This mutation causes the substitution of Gln144 with a stop codon (Q144stop) (**Fig. 3A**). A transformant harboring a genomic DNA fragment bearing At5g47040 showed numerous punctate GFP-fluorescent spots (**Fig. 3B**). This result demonstrates that At5g47040 expression is sufficient to rescue the *apem10* phenotype. An F_1 progeny of a cross between *apem10* and the *lon2-1* T-DNA insertion line showed GFP accumulation in the cytosol, like *apem10*, indicating that *apem10* and *lon2-1* are allelic (**Fig. 3C**). These results demonstrate that *APEM10* is At5g47040/*LON2*.

Subcellular localization of LON2

LON proteases belong to the AAA+ (ATPases associated with various cellular activities) superfamily and are found in bacteria and eukaryotic organelles. Arabidopsis LON2 has 888 amino acid residues and is a typical LON protease, which consists of a conserved LON N-terminal domain, an AAA+ ATPase domain with typical Walker A and B motifs, and a peptidase domain at the C-terminus (Lingard and Bartel 2009, Rigas et al. 2012). LON2 has a C-terminal tripeptide with SKL as the canonical peroxisomal targeting signal 1 (PTS1), and a previous proteomic analysis has identified LON2 in Arabidopsis peroxisomes (Reumann et al. 2009). Observation of transgenic plants expressing *GFP-LON2* and *mRFP1-PTS1* as a peroxisomal marker showed that GFP fluorescence was detected as punctate signals, which merged with monomeric red fluorescent protein (mRFP)–PTS1 (**Fig. 4A**). This result is consistent with the data from proteomic analysis. We separated peroxisome-rich fractions by the subcellular fractionation method (Matsushima

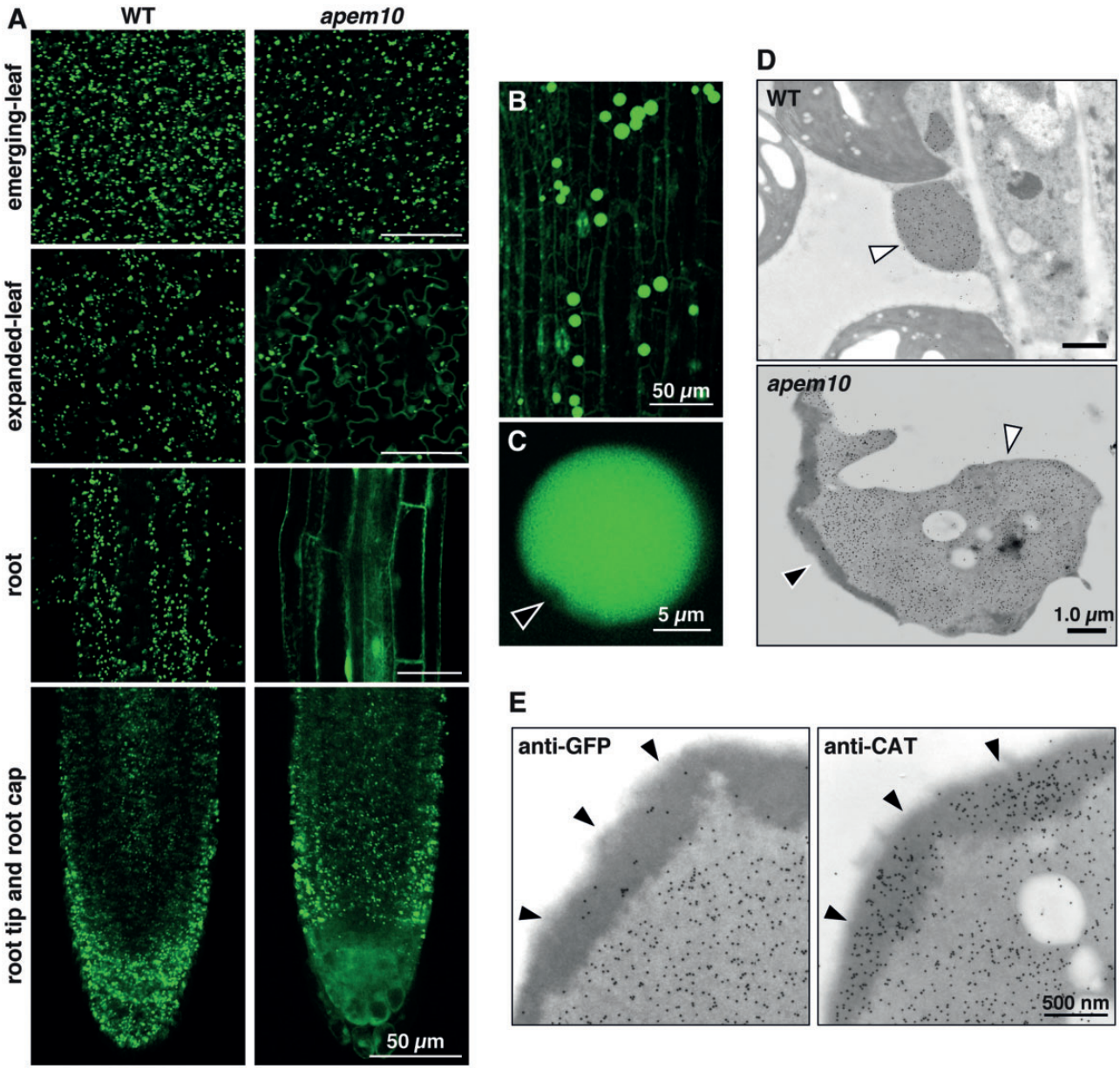

Fig. 2 The *apem10* phenotype. (A) GFP fluorescence patterns of the WT and *apem10*, which express the peroxisome marker GFP–PTS1. The indicated tissues of 2-week-old plants were examined using confocal laser-scanning microscopy. (B) Enlarged peroxisomes in the leaf petiole of the 5-week-old *apem10* mutant. (C) Magnified image of an enlarged peroxisome. The arrowhead indicates the region not visualized with GFP in a peroxisome. (D) Immunoelectron micrographs of the WT and *apem10* using antibodies against GFP. White and black arrowheads indicate peroxisomes and the electron-dense region in peroxisomes, respectively. (E) Immunogold labeling of 5-week-old *apem10* leaves with the GFP (left) or CAT (right) antibodies. Arrowheads indicate the electron-dense regions.

et al. 2003) and subjected the fractions to immunoblot analysis (**Fig. 4B**). A peroxisomal protein, hydroxypyruvate reductase (HPR), was detected mainly in the P1 fraction, with a small amount detected in the P8 fraction. Thus, peroxisomes are considered to be accumulated mainly in the P1 fraction. Some matrix proteins, such as HPR, were detected in the S100 fraction containing the cytosol and vacuole, because such proteins leaked from broken peroxisomes during organelle preparation (**Fig. 4B**). LON2 was mainly detected in P1, with a small amount detected in the P8 and S100 fractions (**Fig. 4B**). This LON2 distribution pattern suggests that LON2 is localized to peroxisomes, confirming the fluorescence pattern of GFP–LON2. To examine the detailed suborganellar localization of LON2 protein, peroxisomes in the P1–P8 fraction were resuspended in low-salt buffer, high-salt buffer and alkaline solution buffer. The peroxisomal membrane protein PEX14 was found in the insoluble fraction even after treatment with alkaline solution. However, the matrix protein HPR was dissolved in low-salt

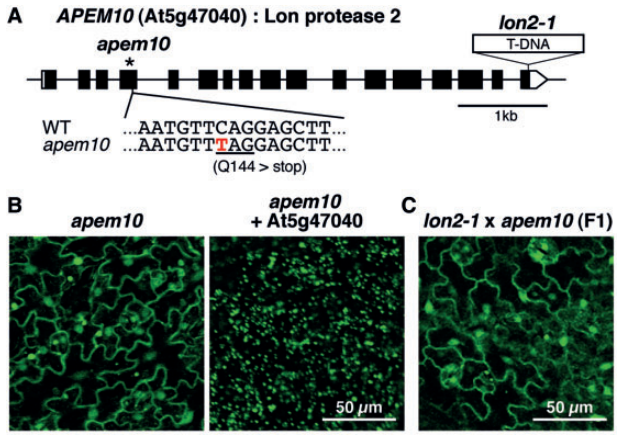

Fig. 3 Identification of the *APEM10* gene. (A) Schematic structure of *APEM10/LON2* gene. The white and black boxes indicate untranslated regions and exons, respectively. The asterisk represents the location of the nucleotide substitution in *apem10*, causing the amino acid substitution of Gln144 with a stop codon. (B) The genomic fragment of At5g47040 restores the GFP fluorescence pattern in *apem10* mutants. Left and right panels show leaf cells of *apem10* and *apem10* transformed with At5g47040, respectively. (C) Test of allelism between *apem10* and *lon2-1* mutants. GFP fluorescence pattern in the F_1 progeny, which were derived from crossing *apem10* with *lon2-1*. Leaves of 2-week-old plants were examined.

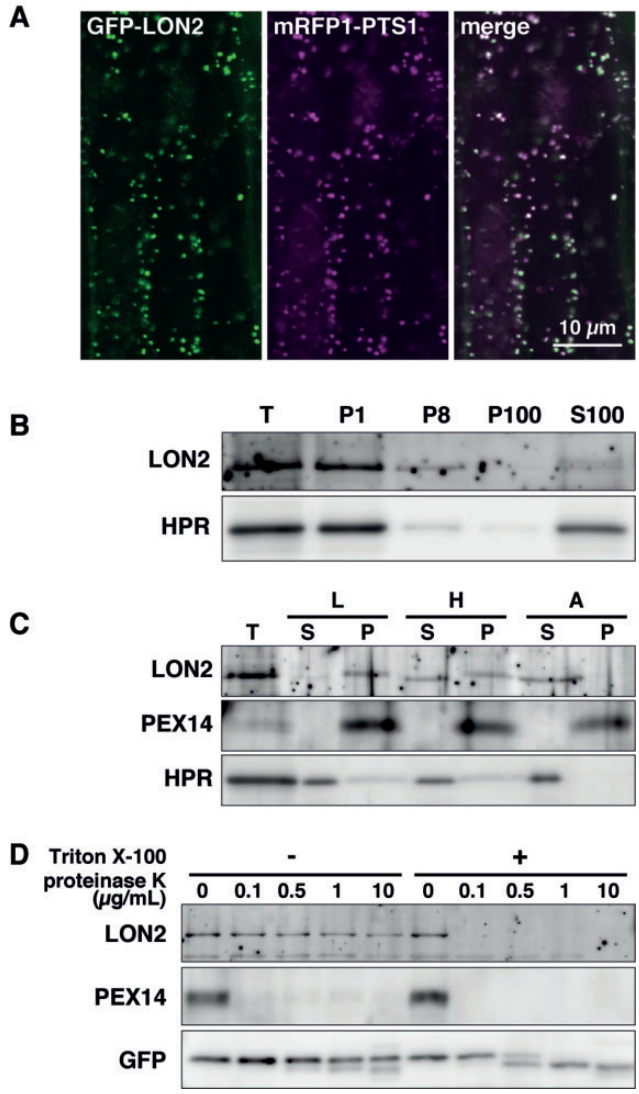

Fig. 4 Subcellular localization of LON2 protein. (A) Fluorescence images of transgenic plants expressing *GFP-LON2* and *mRFP1-PTS1*. Leaves of 2-week-old plants were examined by confocal laser-scanning microscopy. (B–D) Subcellular and suborganellar localization of LON2 in WT plants using immunoblot analysis. (B) The subcellular fraction from 1-week-old WT plants expressing the peroxisome marker GFP–PTS1 was subjected to SDS–PAGE. (C) Isolated peroxisomes in the P1–P8 fractions were resuspended in either low-salt buffer (L; 50 mM NaCl), high-salt buffer (H; 500 mM NaCl) or alkaline solution (A; 0.1 M Na_2CO_3, pH 11). These samples were then centrifuged and separated into soluble (S) and pelletable (P) fractions. T represents total proteins of the isolated peroxisomes before fractionation. (D) Isolated peroxisomes in the P1–P8 fractions were treated with various concentrations of proteinase K in the absence (−) or presence (+) of Triton X-100.

buffer, high-salt buffer and alkaline solution (**Fig. 4C**). LON2 protein is insoluble in low-salt buffer, slightly soluble in high-salt buffer and soluble in alkaline solution (**Fig. 4C**). In addition, LON2 in intact peroxisomes is sensitive to digestion with proteinase K in the presence of Triton X-100 (**Fig. 4D**). Similarly, GFP–PTS1 protein, which is a peroxisomal matrix protein, is degraded with a lower concentration of proteinase K in the presence of Triton X-100 (**Fig. 4D**). These results suggest that LON2 is a peripheral membrane protein, which associates with the membrane from the matrix side.

Absence of LON2 enhances peroxisome degradation by autophagy

To clarify whether LON2 affects the accumulation of peroxisomal proteins, we compared the accumulation levels of peroxisomal proteins in protein extracts from emerging new leaves vs. expanded leaves because the *apem10* phenotype became more noticeable as the tissues grew older (**Fig. 2A**). The amount of peroxisomal membrane protein PEX14, long-chain acyl-CoA synthetase 6 (LACS6) and peroxisomal membrane protein 38 (PMP38), but not peroxisomal ascorbate peroxidase (pAPX), dramatically decreased in the *apem10* mutant (**Fig. 5A**). The decrease in peroxisomal membrane protein levels was more pronounced in expanded leaves than in emerging leaves in *apem10*. However, there was no significant difference in the accumulation of PEX5, the receptor required for peroxisomal protein import, and peroxisomal matrix proteins (such as CAT, HPR and GFP–PTS1) in *apem10* compared with wild-type (WT) plants. In *apem10*, GFP–PTS1 proteins in the cytosol were observed (**Fig. 2A**), so it is possible that other matrix proteins also accumulate in the cytosol. In addition, the low levels of peroxisomal membrane proteins suggest a decrease in peroxisome number. Therefore, we performed indirect immunostaining using antibodies against pAPX to detect peroxisomes and/or peroxisome ghosts. The results revealed that the number of

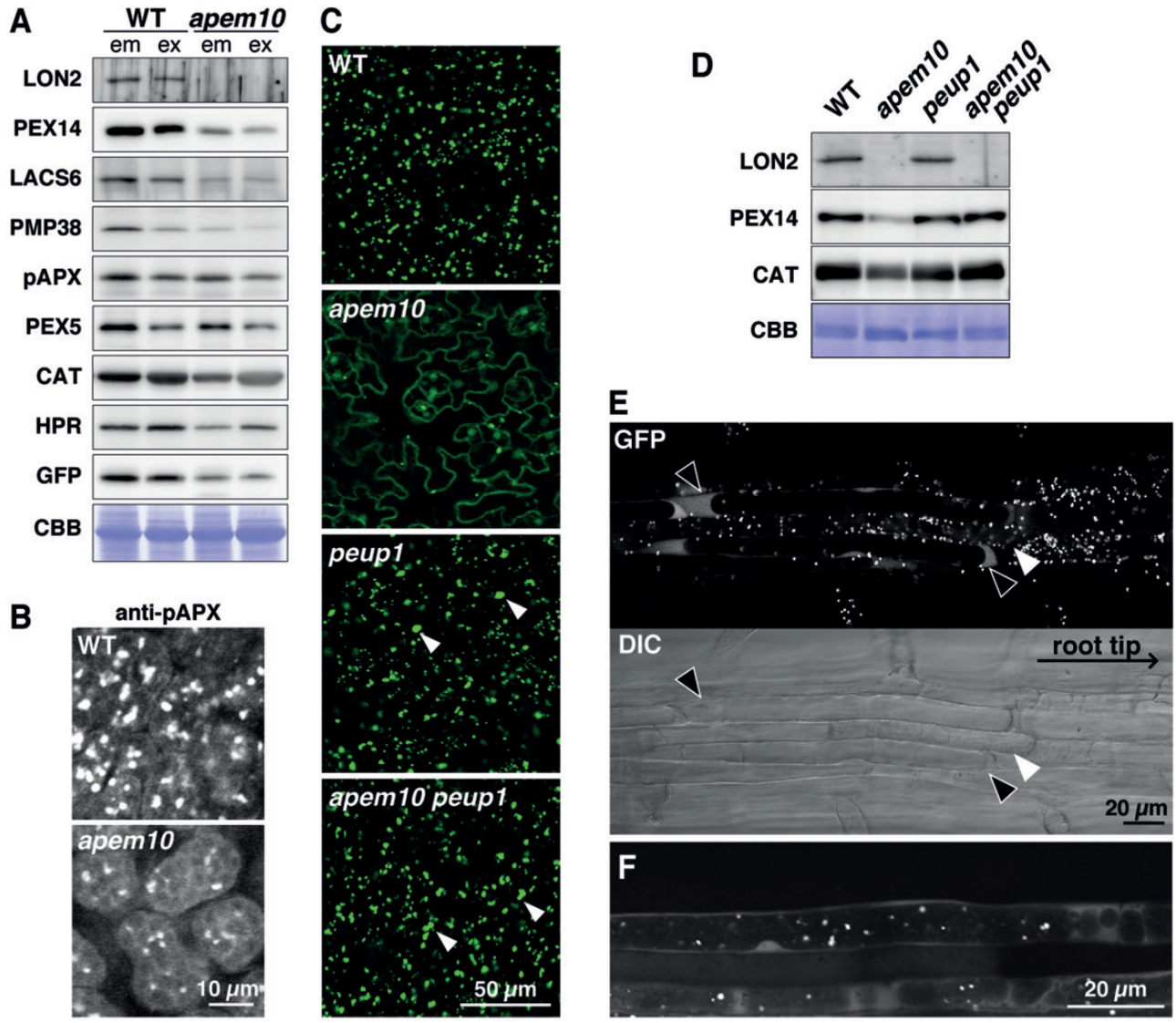

Fig. 5 Reduced number of peroxisomes is rescued by introduction of an autophagy defect in *apem10*. (A) Peroxisomal proteins were immunodetected in extracts from the emerging new leaves (em) or expanded leaves (ex) of 2-week-old WT and *apem10* plants, which express the peroxisome marker GFP–PTS1. Antibodies used in this experiment are indicated on the left. (B) Indirect immunofluorescence analysis using antibodies against pAPX in emerging leaves of 2-week-old WT and *apem10* plants. pAPX signals were detected using antibodies against pAPX and Cy3-labeled secondary antibodies. (C) GFP fluorescence images in WT, *apem10*, *peup1* and *apem10 peup1* plants. Since all plants express the peroxisome marker GFP–PTS1, peroxisomes were visualized with GFP fluorescence. The leaves of 3-week-old plants were examined using confocal laser-scanning microscopy. Arrowheads indicate peroxisomal aggregation. (D) Immunodetection of LON2, PEX14 and CAT in extracts from leaves of 3-week-old plants. (E) GFP fluorescence and DIC (differential interference contast) images of the phenotype-shifting region of roots of 2-week-old *apem10* seedlings. Black and white arrowheads indicate cells showing accumulation of cytosolic GFP and containing numerous peroxisomes, respectively. (F) GFP fluorescence images of the phenotype-shifting region in *apem10*. Seven-day-old seedlings were transferred to liquid growth medium containing 1 μM ConA and grown for 1 d in the light, and then observed by confocal laser-scanning microscopy.

vesicles labeled with pAPX antibodies decreased and pAPX signals were dispersed in the cytosol or in cellular compartments, which may be subdomains of the rough ER (**Fig. 5B**) (Lisenbee et al. 2003). However, the expression of *PEX14* was not lower in *apem10* than in the WT (**Supplementary Fig. S2**), supporting the notion that the decrease in the amount of PEX14 in the *apem10* mutant was caused by degradation of peroxisomes rather than by down-regulation of gene expression. These results, along with the observation of the decrease in punctate GFP signals in the *apem10* mutant (**Fig. 2A**), suggest that peroxisomes might be degraded in the *apem10* mutant.

Previous studies have shown that oxidized or excess peroxisomes are degraded by autophagy in yeast, mammals and plants (Iwata et al. 2006, Aksam et al. 2007, Shibata et al. 2013). To clarify whether the number of peroxisomes in *apem10* is reduced by autophagy, we generated a double

mutant by crossing *apem10* with *peroxisome unusual positioning 1* (*peup1*), in which peroxisome degradation is arrested due to the defect of autophagy-related 2 (ATG2) (Shibata et al. 2013). In the *apem10 peup1* double mutant, cytosolic GFP fluorescence disappeared and the peroxisome number increased compared with *apem10* (**Fig. 5C**). The aggregation of peroxisomes was frequently observed, which also occurs in *peup1* (in which oxidized peroxisomes accumulate as aggregates) (Shibata et al. 2013). As the peroxisome number increased in the double mutant, the amount of PEX14 also increased to the level of the WT (**Fig. 5D**). Additionally, growth arrest in *apem10*, which was already reported in a previous study (Lingard and Bartel 2009), was rescued in the double mutant (**Supplementary Fig. S3**). Mutants defective in autophagy-related genes show an early senescence phenotype, especially under nutrient-deficient conditions. Similarly, the double mutant displayed early senescence in its rosette leaves (**Supplementary Fig. S3**), indicating that autophagy is repressed in the double mutant. These results demonstrate that the decrease in peroxisome number is caused by accelerated peroxisome degradation that occurs via autophagy.

We then examined whether the decrease in peroxisome number is responsible for cytosolic GFP accumulation in *apem10*. It was easy to assay the *apem10* phenotype in root cells because these cells exhibited various gradations of phenotype along the developmental lineage; numerous peroxisomes remained in young cells near the root tip, whereas the peroxisome number was dramatically reduced in the upper cells of the root. **Fig. 5E** shows the border region where adjacent cells exhibiting each phenotype were observed. In this region, cells containing numerous peroxisomes began to exhibit cytosolic GFP accumulation over time. To reveal the relationship between autophagy and the shift in the *apem10* phenotype, *apem10* seedlings were treated with the vacuolar H^+-ATPase inhibitor concanamycin A (ConA), which is used to detect autophagy since it inhibits the degradation of autophagic bodies in the vacuole (Yoshimoto et al. 2004). In cells of the phenotype-shifting region of ConA-treated *apem10* roots, peroxisome-like vesicles were detected in the vacuole. At this point, dim GFP fluorescence was observed in the cytosol, revealing initiation of the accumulation of GFP protein in the cytosol (**Fig. 5F**). These results suggest that peroxisomes are degraded by autophagy before the cells exhibit cytosolic GFP fluorescence. Therefore, GFP–PTS1 protein accumulates in the cytosol due to a lack of peroxisomes, which could function as containers.

LON2 is responsible for the functional transition of peroxisomes, and this process is coordinated with peroxisome degradation by autophagy

During post-germinative growth, peroxisomal functions are rapidly exchanged. Glyoxysomal enzymes required for lipid metabolism become less abundant and are substituted with leaf peroxisomal enzymes that contribute to photorespiration after the plant is exposed to light (Beevers 1979). During this functional transition, degradation of glyoxysomal proteins occurs immediately. To analyze another aspect of LON2 function, we focused on the relationship among LON2 functions, autophagy and the peroxisomal functional transition of glyoxysomes to leaf peroxisomes. Immunoblot analysis showed that glyoxysomal enzymes such as malate synthase (MS), isocitrate lyase (ICL) and thiolase were highly accumulated in seedlings grown in continuous darkness (**Fig. 6A**, '4D'), and these enzymes were degraded after illumination (**Fig. 6A**, '4D1L', '4D2L' and '4D3L') in WT plants. The amount of the leaf peroxisomal enzyme HPR increased, whereas illumination did not alter the amount of the membrane protein PEX14. In the *apem10* mutant, the level of glyoxysomal proteins was lower than in WT plants, even in the dark. This decrease in *apem10* may be caused by accelerated peroxisomal degradation by autophagy. In the *apem10* and *peup1* mutants, the amount of glyoxysomal and leaf peroxisomal proteins decreased and increased, respectively, which also occurred in WT plants. However, ICL and MS still remained in the *apem10 peup1* double mutant. Aggregates of peroxisomes, which contain oil bodies, are present in mesophyll cells of etiolated cotyledons (Hayashi et al. 2001); these aggregates disappeared and peroxisomes became present as independent vesicles after the functional transition (**Fig. 6B**, 'WT'). In *apem10* cotyledons, the number of peroxisomes in the mesophyll cells decreased. In the *peup1* and *apem10 peup1* mutants, peroxisome aggregates remained in the mesophyll cells, indicating that clearance of these aggregates requires autophagy (**Fig. 6B**). These results implicate that glyoxysomal proteins are degraded by two independent degradation pathways, i.e. the LON2- and autophagy-dependent pathways. In contrast to ICL and MS, thiolase was not degraded in the *peup1* mutant (**Fig. 6A**), indicating that thiolase is not a substrate of LON2, and that it is degraded by autophagy during the peroxisomal functional transition.

The chaperone function of LON2 suppresses peroxisome degradation by autophagy, while its protease function interferes with this suppression

LON proteases play roles as multifunctional enzymes and contribute to the degradation of oxidized and damaged proteins in bacteria and organelles in eukaryotic cells (Wagner et al. 1994, Aksam et al. 2007, Bayot et al. 2010, Bissonnette et al. 2010, Bartoszewska et al. 2012). Moreover, the AAA+ ATPase domain, which probably functions with the N-terminal domain, provides the mechanical power needed to unfold substrate proteins; thus, LON proteins act as a molecular chaperone (Rep et al. 1996, Van Melderen and Gottesman 1999, Gur and Sauer 2009, Bissonnette et al. 2010, Bartoszewska et al. 2012, Rigas et al. 2012). To investigate which domain in LON2 is essential for its function. We generated two mutant forms of LON2 containing amino acid substitutions: Lys414 to alanine (LON2[K414A]) and Ser783 to alanine (LON2[S783A]) (**Fig. 7A**). Lys414 is present in the ATP-binding site of the

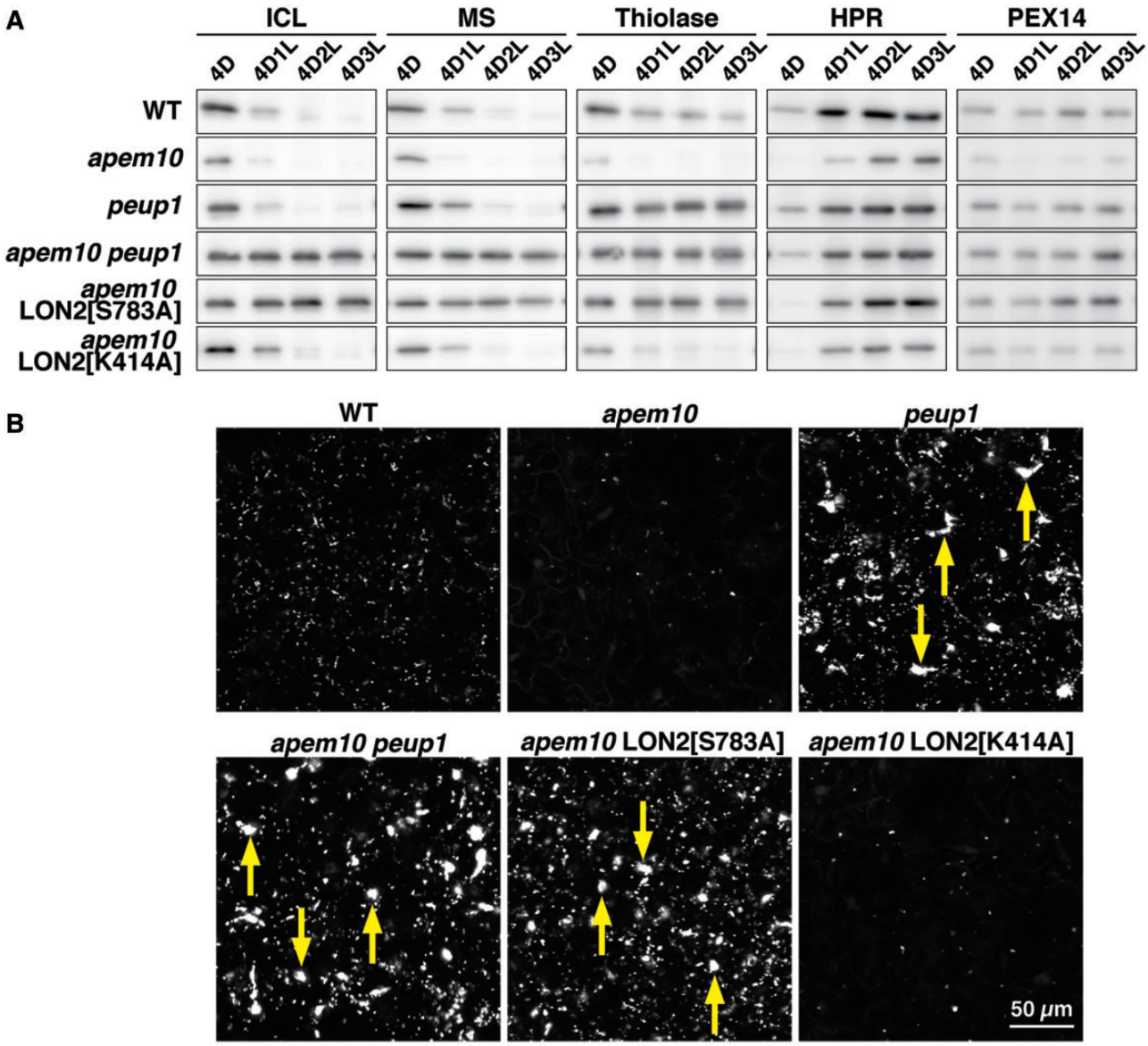

Fig. 6 Relationship between LON2 and autophagy during the functional transition of peroxisomes. (A) Seedlings of WT, *apem10*, *peup1*, *apem10 peup1* double mutants and LON2 transformants were grown in continuous darkness for 4 d (4D) and then transferred to continuous illumination for 1 d (4D1L), 2 d (4D2L) or 3 d (4D3L). Total extracts prepared from cotyledons were subjected to immunoblotting using antibodies as indicated above. (B) Z-projection of GFP fluorescence images of mesophyll cells from 4D3L seedlings. Arrows indicate aggregates of peroxisomes.

Walker A motif of the AAA+ ATPase domain, and the K414A mutation is expected to arrest the binding of ATP to LON2. Ser783 is a conserved residue at the active center of the peptidase domain, in which the substitution of Ser783 by alanine inactivates peptidase activity. Two mutated and WT LON2 (LON2[WT]) constructs were expressed in the *apem10* mutant under the control of the *LON2* promoter (**Fig. 7A**). Lines expressing adequate amounts of LON2 protein were selected for further analysis (**Fig. 7B**). In LON2[WT]-transformed *apem10*, GFP fluorescence was observed in peroxisomes and not in the cytosol, which was also observed in WT plants (**Fig. 7C**). Interestingly, the introduction of LON2[S783A], but not LON2[K414A], was able to rescue the *apem10* phenotype (**Fig. 7C**). In addition, the number of peroxisomes in *apem10* LON2[S783A] was higher than that of WT plants (**Fig. 7D**). During the functional transition, in *apem10* LON2[S783A], the glyoxysomal proteins ICL, MS and thiolase accumulated as they had in the *apem10 peup1* double mutant (**Fig. 6A**), and the peroxisome aggregates remained in the mesophyll cells (**Fig. 6B**). In *apem10* LON2[K414A], the changes in the amounts of glyoxysomal and leaf peroxisomal proteins were similar to those in *apem10*, and the number of peroxisomes in the mesophyll cells was reduced, as in *apem10*. These results indicate that the suppression of peroxisome degradation by autophagy requires the chaperone domain but not the peptidase domain. Notably, the number of peroxisomes in the

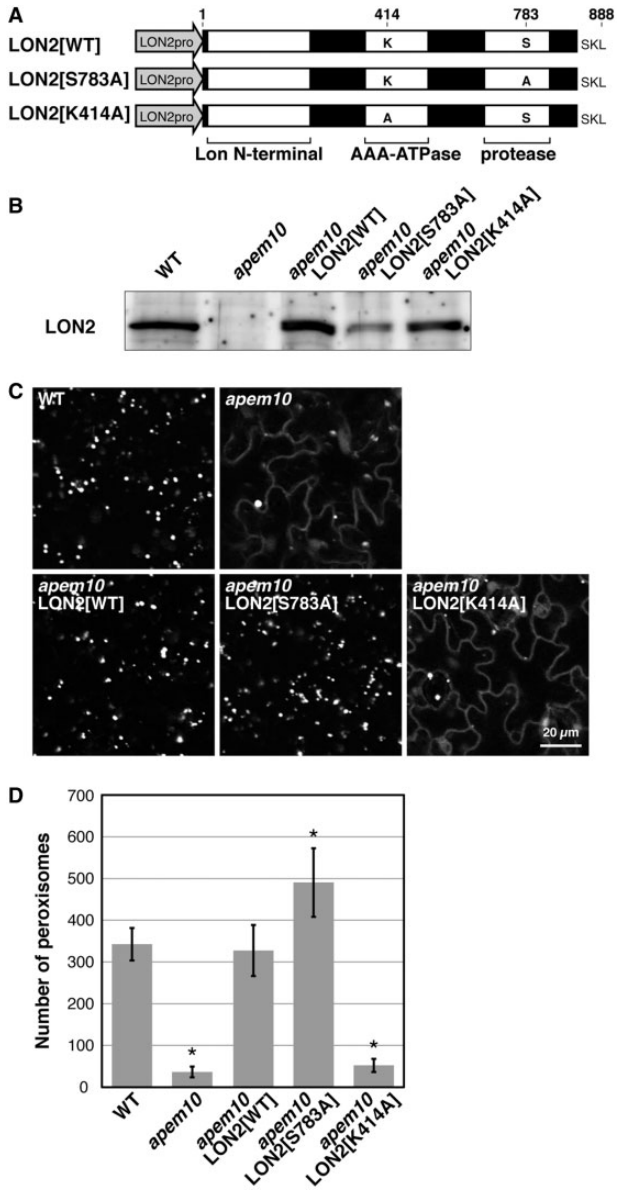

Fig. 7 Suppression of autophagy requires the chaperone domain of LON2. (A) Schematic structures of *LON2* constructs used in this experiment. These cDNAs were expressed under the control of the *LON2* promoter. (B) Immunodetection of LON2 in extracts of 1-week-old transgenic plants was carried out to estimate the accumulation of WT and modified LON2 proteins. (C) GFP fluorescence images of expanded leaves in WT plants, the *apem10* mutant and the LON2 transformant, which expresses modified *LON2* genes in the *apem10* background. (D) Quantification of peroxisome number. The GFP-fluorescent spots in a $5.04 \times 10^4\ \mu m^2$ area in images from leaves of 2-week-old plants were counted. Asterisks indicate a significant difference ($P < 0.05$, Welch's *t*-test) when compared with WT plants. The error bars indicate the SD ($n = 4$).

apem10 LON2[S783A] plants was higher than that in WT plants in both rosette leaves and greening cotyledons (**Figs. 6B**, **7D**), and *apem10* LON2[S783A] shows accumulation of glyoxysomal proteins like the *apem10 peup1* double mutant after illumination (**Fig. 6A**). These results indicate that the peptidase domain of LON2 reduced the effect of the chaperone function on the suppression of autophagy.

Discussion

The *apem10* mutant showed cytosolic accumulation of GFP–PTS1 protein. At first, we speculated that *APEM10* encodes a crucial factor for peroxisomal protein transport, such as APEM2/PEX13, APEM4/PEX12 or APEM9 (Mano et al. 2006, Goto et al. 2011). However, our results show that the number of peroxisomes was reduced in the *apem10* mutant, and that the *apem10 peup1* double mutant displayed an increased number of peroxisomes along with the disappearance of cytosolic GFP fluorescence, even though the double mutant had a defective *LON2* gene (**Fig. 5**). Based on these results, we conclude that peroxisomal proteins accumulate in the cytosol due to the acceleration of peroxisome degradation in *apem10*. We found that the amount of peroxisomal membrane proteins, but not matrix proteins, was dramatically reduced in *apem10* (**Fig. 5A**). According to the expression profiles of these genes in rosette leaves that were obtained from the eFP browser (http://bbc.botany.utoronto.ca/efp/cgi-bin/efpWeb.cgi), the expression levels of membrane proteins, except for pAPX, were one order of magnitude lower than those of matrix proteins (**Supplementary Table S2**). Due to the high expression levels of matrix proteins, the large amounts of newly synthesized proteins may have concealed the decrease in protein levels due to degradation. However, synthesized proteins, such as GFP–PTS1 proteins, may have accumulated in the cytosol (**Fig. 2**). The expression level of pAPX was 3.6–5.7 times higher than that of the other membrane proteins. Since pAPX resides within a subdomain of the rough ER before it is sorted to the peroxisomes (Lisenbee et al. 2003), newly synthesized pAPX may have accumulated in the rough ER under our conditions, in which peroxisomes were degraded by autophagy. It is known that autophagy in plant cells degrades cellular components in response to environmental signals such as nitrogen starvation (Yoshimoto et al. 2004). The enhancement of the *apem10* phenotype under nitrogen-starved conditions (**Supplementary Fig. S1**) may be a corollary of the additional degradation of peroxisomes by starvation-induced autophagy.

Four *LON* genes, *LON1–LON4*, are present in the Arabidopsis genome. LON1 protein is found in the mitochondrial inner membrane fraction. The loss of LON1 causes a reduction in the activities of respiratory chain complexes and enzymes of the tricarboxylic acid (TCA) cycle, as well as abnormal morphology of the mitochondria (Rigas et al. 2009). Proteomic analysis using the Arabidopsis *lon1* mutant suggested that LON1 is involved in the assembly of the mitochondrial membrane protein complexes (Solheim et al. 2012). LON3 is regarded as a pseudogene, since its transcript is absent in the EST (expressed sequence tag) database (Ostersetzer et al. 2007). LON4 is dual targeted to mitochondria and plastids, and plastid-targeted

LON4 is attached to the stromal side of the thylakoid membrane (Ostersetzer et al. 2007). LON2 has a canonical PTS and was identified in the proteome of isolated peroxisomes (Reumann et al. 2009). The *lon2* mutants show defects in peroxisomal functions (Lingard and Bartel 2009). This study shows that LON2 is present as a peripheral membrane protein (**Fig. 4C, D**). Mammalian peroxisomal LON protease interacts with the peroxisomal membrane protein PMP70 (Omi et al. 2008). Since LON proteases can act as molecular chaperones, we expect that LON2 is involved in the stability, assembly and/or conformation of peroxisomal membrane proteins. In Arabidopsis, a defect in PMP38 causes a failure of peroxisome division, resulting in the enlargement of peroxisomes (Mano et al. 2011). It is possible that PMP38 exists in membranes in an unfolded or unstable state, and that peroxisomes are not able to divide in *apem10*. The failure of peroxisome proliferation and the acceleration of autophagy may cause a substantial decrease in the peroxisome number and the enlargement of peroxisomes in *apem10*. The enlargement of peroxisomes was suppressed by the arrest of photorespiration in *apem10* (**Supplementary Fig. S1**). H_2O_2 in peroxisomes is produced during photorespiration. Therefore, LON2 might be required for the maintenance of peroxisomal proteins, including PMP38, under this stressful condition.

LON proteases, which belong to the AAA+ superfamily, are conserved in various organisms, including bacteria, and are localized in various organelles in eukaryotic cells (Gur and Sauer 2009). Functional LON protein is present as a homohexamer or homoheptamer (Stahlberg et al. 1999, Rotanova et al. 2006, Duman and Löwe 2010, Bartoszewska et al. 2012), and each subunit consists of an N-terminal domain, an AAA+ ATPase domain (which provides mechanical power and acts as a molecular chaperone with the N-terminal domain) and a peptidase domain. LON proteases are involved in cellular or organellar homeostasis. For example, a LON protease plays a major role in the clearance of misfolded and damaged proteins in *Escherichia coli*, and the mitochondrial LON protease PIM1 degrades misfolded and oxidatively damaged proteins in yeast (Wagner et al. 1994, Bayot et al. 2010, Bissonnette et al. 2010). Peroxisomal LON protease is also thought to be involved in protein degradation. Peroxisomal LON interacts with peroxisomal proteins and degrades target proteins in mammal, yeast and the filamentous fungus *Penicillium chrysogenum* (Aksam et al. 2007, Omi et al. 2008, Yokota et al. 2008, Bartoszewska et al. 2012). The AAA+ superfamily domain has ATP-dependent unfolding activity, which disassembles protein complexes and promotes disaggregation (Sauer et al. 2004). LON proteases are involved in protein unfolding and refolding in various organisms (Goldberg et al. 1994, Rep et al. 1996, Van Melderen and Gottesman 1999, Bissonnette et al. 2010, Gur et al. 2012). Recently, Bartoszewska et al. showed that peroxisomal LON in *P. chrysogenum* has chaperone activity in vitro (Bartoszewska et al. 2012).

Recently, we demonstrated that autophagy mutants accumulate peroxisome aggregates consisting of peroxisomes that had been oxidized by excess H_2O_2. This result indicates that autophagy serves as a quality control mechanism via selective elimination of damaged peroxisomes in the plant cell (Shibata et al. 2013). In this study, we demonstrated the existence of two degradation systems, namely the LON2- and autophagy-dependent pathways (**Fig. 6**). During the preparation of this manuscript, Farmer et al. reported similar results, i.e. LON2 is responsible for matrix protein turnover with autophagy (Farmer et al. 2013), confirming that double processes exist for the degradation of peroxisomal proteins. In this study, we could provide an important clue concerning the molecular mechanisms of autophagy regulation, i.e. the chaperone function of LON2 suppresses autophagy and its protease function interferes with this suppression. Peroxisomal degradation is regulated by cross-talk between the multifunctions of LON2 and autophagy, and this process contributes to peroxisomal quality control and is required for the functional transition during post-germinative growth. As shown in **Fig. 2**, the *apem10*/*lon2* mutant accumulated peroxisomal matrix proteins in the cytosol, as previously reported (Lingard and Bartel 2009, Farmer et al. 2013). In these studies, the authors concluded that LON2 is involved in the machinery required for peroxisomal protein transport. In this study, however, we demonstrated that peroxisomal proteins accumulate in the cytosol due to degradation of peroxisomes by autophagy. Based on these data and the current results, we propose that the functional transition proceeds as follows: (i) glyoxysomal proteins are removed by the protease activity of LON2 inside peroxisomes concomitantly with the import of newly synthesized leaf peroxisomal proteins, which is in agreement with the one-population hypothesis (**Fig. 1A**); and (ii) pre-existing oxidized glyoxysomes, which are exposed to ROS when functioning, are eliminated by autophagy, which is in agreement with the two-population hypothesis (**Fig. 1B**). In this process, LON2 also suppresses autophagy to allow some glyoxysomes to escape from degradation. In the absence of LON2 function, peroxisomes are rapidly degraded. As mentioned in **Fig. 1C**, this new model comprises both one-population and two-population hypotheses. To understand how LON2 regulates autophagy, we propose two direct and indirect mechanisms: (i) LON2 directly interacts with a factor that regulates autophagy; or (ii) LON2 maintains peroxisomal proteins to keep the peroxisomes in proper working order, allowing the peroxisomes to elude recognition by autophagy (**Fig. 8**). These two mechanisms should be addressed in future studies.

In mammalian cells, LON protease has the ability to interact with β-oxidation enzymes and to degrade them in proliferated peroxisomes induced by di-(2-ethyl-hexyl)phthalate (DEHP) treatment (Omi et al. 2008, Yokota et al. 2008). Also, most peroxisomes induced by DEHP are degraded by autophagy (Iwata et al. 2006), suggesting that the cooperation of LON protease and autophagy is involved in the quality control of mammalian peroxisomes. On the other hand, in the methylotrophic yeast *Hansenula polymorpha*, a defect in peroxisomal LON protease (Pln) causes a slight increase in peroxisome

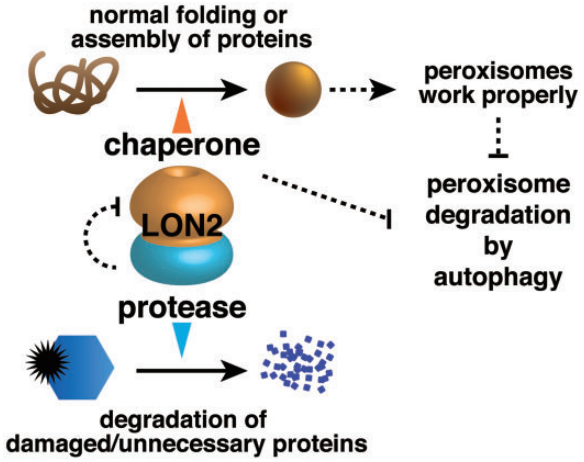

Fig. 8 A model for the coordinated regulation of peroxisomal quality control by multiple LON2 functions and autophagy. The protease function of LON2 is required for degradation of unnecessary proteins, whereas chaperone function is involved in normal folding or assembly of proteins that may contribute to proper action of peroxisomes. This study shows that the chaperone function of LON2 suppresses autophagy via a direct or indirect contribution, and that its protease function interferes with this chaperone function.

number, as is also the case in *atg1* and *pln atg1* double-mutant cells (Aksam et al. 2007). In the filamentous fungus *P. chrysogenum*, no difference in peroxisome distribution between WT and *pln* cells is observed (Bartoszewska et al. 2012). These reports suggest that the mechanisms of the regulation of peroxisome number by LON protease and autophagy differ among organisms. Intriguingly, electron microscopy of *pln* mutant cells of both fungi shows electron-dense inclusions in the peroxisomal lumen, which consist of protein aggregates (Aksam et al. 2007, Bartoszewska et al. 2012). In rat liver cells, the LON isoform is mainly associated with the electron-dense inclusions in the peroxisomal matrix (Kikuchi et al. 2004). These reports, combined with our observation that the peroxisomes in the *apem10* mutants also contain electron-dense regions (**Fig. 2D, E**), suggest that the function of LON family proteins in the removal of protein aggregates is conserved in various organisms.

LON proteases are involved in protein unfolding and refolding in various organisms (Goldberg et al. 1994, Rep et al. 1996, Van Melderen and Gottesman 1999, Bissonnette et al. 2010, Gur et al. 2012, Bartoszewska et al. 2012). However, the importance of the chaperone function of LON proteins in biological processes was previously unclear. Our approach, in which we dissected the two functions of LON2, revealed that the chaperone function of this protein, but not its peptidase activity, suppresses autophagy, although it is still unclear whether LON2 contributes directly or indirectly to the regulation of autophagy. Intriguingly, the peptidase function of LON2 interferes with its chaperone function, indicating that intramolecular modulation between the proteolysis and chaperone functions of LON2 regulates degradation of peroxisomes by autophagy (**Fig. 8**). Since LON protease and autophagy are conserved in a wide range of organisms, and since LON protease are localized in various organelles, the results of our study should help to increase our understanding of quality control mechanisms in other organelles and organisms.

Materials and Methods

Plant materials and growth conditions

The GFP–PTS1 transgenic plants and the *apem10* mutant were derived from the Columbia background (Mano et al. 2002, Mano et al. 2004). The knockout line containing a T-DNA insertion in the At5g47040 locus, SALK_128438 (*lon2-1*), was obtained from the Arabidopsis Biological Resource Center (ABRC) (http://abrc.osu.edu/). To examine the relationship between its phenotype and genotype, the presence of the T-DNA insertion was confirmed by PCR using gene-specific primers with the T-DNA specific LB-1 primer (**Supplementary Table S1**). All seeds were surface-sterilized in 2% (v/v) NaClO, 0.02% (v/v) Triton X-100 and germinated on growth medium containing 2.3 mg ml^{-1} Murashige and Skoog salts (Wako), 0.5 μg ml^{-1} MES-KOH (pH 5.7) and 0.8% (w/v) agar (INA) with or without 1% (w/v) sucrose. Germination was induced by incubating the seeds for 48 h at 4°C and then transferring them to 22°C under continuous light. Since the *apem10* mutant showed severe germination defects, all seed coats were nicked to accelerate seed coat rupturing (Footitt et al. 2006, Kanai et al. 2010).

Confocal microscopy

Tissues from plants were examined using an LSM510META confocal laser-scanning microscope (Carl Zeiss), as previously described (Mano et al. 2002). Z-projection images of mesophyll cells in **Fig. 6B** were produced using the following steps. First, a Z-stack image comprising five slices was produced. The first slice was obtained, showing the top surface of the epidermal cells, and the other slices were obtained using 8 μm steps from the first slice. To produce an image of the mesophyll cells, the third to fifth images were used for Z-projection with maximum intensity projection using ImageJ software (NIH, http://rsb.info.nih.gov/ij), since the first and second slices contained signals from epidermal cells.

Map-based cloning and identification of *APEM10*

The *apem10* mutant, which was backcrossed three times with the parental GFP–PTS1 transgenic plant, was crossed with another accession, Landsberg *erecta*, to produce F_1 and, subsequently, F_2 progeny. A total of 180 F_2 progeny expressing the *apem10* phenotype were scored according to their genetic background, as determined using a series of cleaved amplified polymorphic sequence (CAPS) and simple sequence length polymorphism (SSLP) markers (Konieczny and Ausubel 1993, Bell and Ecker 1994). Rough mapping showed the location of the *APEM10* locus between the DFR and LFY3 markers on chromosome 5. Several sets of CAPS and SSLP markers were

used for fine mapping, according to sequences available in the Monsanto Arabidopsis Polymorphism Collection (http://www.Arabidopsis.org/browse/Cereon/), and NARAMAP markers, which were kindly provided by M. Tasaka and M. Morita at the Nara Institute of Science and Technology (Toyota et al. 2011). Fine mapping identified the *APEM10* locus between the MPL12 and K14A3 BAC clones, which contains 106 predicted genes. The nucleotide substitution in At5g47040 revealed it to be a possible candidate for the *APEM10* gene.

To confirm that the correct gene was identified, the *APEM10* genomic fragment, which included a 2.0 kb upstream region and a 0.5 kb downstream region, was cloned into pCR8/GW/TOPO (Invitrogen) using specific primers (**Supplementary Table S1**), and the insert was transferred into the binary vector pGWB1 (Nakagawa et al. 2007) using the Gateway LR recombination method (Invitrogen). The construct was transformed into *Agrobacterium tumefaciens* strain C58C1Rif^R and then introduced into *apem10* plants using the floral dip method (Clough and Bent 1998).

Plasmid construction

The *LON2* cDNA fragments, which were conjugated with *att*B1 and *att*B2 sequences at their 5′ and 3′ ends, respectively, were amplified by PCR with gene-specific primer sets (**Supplementary Table S1**) and cloned into the entry vector pDONR221 (Invitrogen) using the Gateway BP recombination method (Invitrogen). *LON2* cDNA clones containing the K414A (LON2[K414A]) and S783A (LON2[S783A]) mutations were prepared by PCR-based site-directed mutagenesis with *Pfu* Turbo DNA polymerase (Stratagene) and the specific primer set (**Supplementary Table S1**). The *LON2* promoter, which included a 2.0 kb upstream region and start codon, was cloned into entry vector pDONR P4-P1R (Invitrogen) using specific primers (**Supplementary Table S1**) to generate pDONRP4-P1R/LON2pro.

For complementation analysis of *apem10*, each *LON2* cDNA fragment (LON2[WT], LON2[K414A] and LON2[S783A]), which was cloned into pDONR221, was transferred into the destination vector R4pGWB601 (Nakamura et al. 2010) with pDONRP4-P1R/LON2pro to generate binary vectors expressing modified *LON2* cDNAs under the control of the *LON2* promoter. The construct was transformed into *A. tumefaciens* strain C58C1Rif^R and then introduced into *apem10* plants using the floral dip method (Clough and Bent 1998).

Immunoblot analysis

To extract total proteins, Arabidopsis seedlings were homogenized with extraction buffer containing 20 mM Tris–HCl, pH 6.8, 10% (v/v) β-mercaptoethanol, 2% (w/v) SDS and 24% (v/v) glycerol. The homogenates were centrifuged at 20,000 × *g* for 10 min at 4°C, and the supernatants were collected. The concentration of extracted proteins was estimated using a protein assay kit (Bio-Rad) with bovine γ-albumin as a standard. The proteins were separated by SDS–PAGE and transferred to a polyvinylidene fluoride membrane (Millipore) in a semi-dry electroblotting system. Immunodetection was performed on the membrane using rabbit antibodies raised against LON2 (1 : 2,000 dilution), PEX14 (1 : 7,000 dilution), ACS6 (1 : 5,000 dilution), PMP38 (1 : 5,000 dilution), pAPX (1 : 8,000 dilution), PEX5 (1 : 3,000 dilution), CAT (1 : 8,000 dilution), HPR (1 : 4,000 dilution), MS (1 : 3,000 dilution), ICL (1 : 4,000 dilution), thiolase (1 : 15,000 dilution) and GFP (1 : 3,000 dilution), and immunoreactive bands were detected by monitoring the activity of a horseradish peroxidase-conjugated antibody against rabbit IgG (ECL system; GE Healthcare BioSciences).

Indirect immunostaining

Leaves from 2-week-old plants were analyzed as described previously (Yamada et al. 2008). An antibody against pAPX (1 : 2,000 dilution) and the secondary antibody Cy3-conjugated anti-rabbit IgG (1 : 1,000 dilution) were used.

Subcellular fractionation and analysis of isolated peroxisomes

To separate the peroxisome-rich fractions, the subcellular fractionation method was performed according to Matsushima et al. (2003), with several modifications. Briefly, 1-week-old seedlings (0.5–1.0 g) were chopped with a razor blade in a Petri dish on ice in 1.5–3.0 ml of chopping buffer containing 50 mM HEPES-NaOH (pH 7.5), 1 mM EDTA and 0.4 M sucrose. The homogenate was filtered through a cell strainer (BD Bioscience) with brief centrifugation. An aliquot of the filtrate was used as the total fraction. A 1 ml aliquot of the filtrate was centrifuged at 1,000 × *g* at 4°C for 20 min. The pellet was resuspended in 1 ml of chopping buffer and was designated as the P1 fraction. The supernatant was centrifuged again at 8,000 × *g* at 4°C for 20 min. The pellet was resuspended in 1 ml of chopping buffer and was designated as the P8 fraction. The supernatant was ultracentrifuged at 100,000 × *g* at 4°C for 1 h. The pellet was resuspended in 1 ml of chopping buffer and was designated as the P100 fraction, and the supernatant was designated as the S100 fraction. Each fraction was subjected to SDS–PAGE, and the relative distribution of peroxisomal proteins in each fraction was compared using immunoblot analysis with specific antibodies against HPR. HPR was detected in the P1 and P8 fractions. Therefore, the P1 and P8 fractions were used as the peroxisome-rich fractions.

The filtrated homogenates were centrifuged at 8,000 × *g* at 4°C for 20 min, and the pellet was designated as the P1–P8 fraction. Peroxisomes in the P1–P8 fraction were resuspended in either low-salt buffer (10 mM HEPES-KOH, pH 7.2, 1 mM EDTA and 50 mM NaCl), high-salt buffer (10 mM HEPES-KOH, pH 7.2, 1 mM EDTA and 500 mM NaCl) or alkaline buffer (0.1 M Na_2CO_3, pH 11) for 1 h at 4°C, and the solution was then centrifuged at 100,000 × *g* at 4°C for 30 min to separate it into the supernatant and pellet. In some experiments, peroxisomes in the P1–P8 fraction were incubated with chopping buffer containing an appropriate concentration of

proteinase K for 30 min at 4°C in the presence or absence of 5% (v/v) Triton X-100. The reactions were terminated by the addition of 1 mM phenylmethylsulfonyl fluoride.

Immunoelectron microscopy

Immunocytochemical procedures were, essentially, as described previously (Nishimura et al. 1993). The leaves of 5-week-old plants containing enlarged peroxisomes were screened using fluorescence microscopy and employed as a sample. An antibody against GFP (1 : 1,000 dilution) and CAT (1 : 5,000 dilution), as well as IgG–gold (15 nm; GE Healthcare, 1 : 50 dilution), were used in this experiment.

Accession numbers

Sequence data from this article can be found in the GenBank/EMBL data libraries under the following accession numbers: *LON2* (At5g47040) and *ATG2* (At3g19190). The GenBank accession number for the knockout line described in this article is SALK_128438 (*lon2-1*).

Supplementary data

Supplementary data are available at PCP online.

Funding

This study was supported by the Japan Society for the Promotion of Science (JSPS) [Grant-in-Aid for Scientific Research on Innovative Areas 'Environmental sensing of plants: Signal perception, processing and cellular responses' (grant No. 22120007) and Grant-in-Aid for Scientific Research on Priority Areas 'Organelle Differentiation as the Strategy for Environmental Adaptation in Plants' (No. 16085209) to M.N.; Grant-in-Aid for Young Scientists 'B' (No. 18770039) to S.M.]; the Ministry of Education, Culture, Sports, Science and Technology (MEXT) KAKENHI [Grant-in-Aid for Young Scientists 'Start-up' (No. 25891028) to S.G.-Y.]; JSPS KAKENHI [Research Fellowship for Young Scientists (No. 22-9) to S.G.-Y.]; the Center for the Promotion of Integrated Sciences (CPIS) of Sokendai.

Acknowledgments

We thank T. Nakagawa for providing the Gateway vectors, R.Y. Tsien for providing the *mRFP1* clone, C. Nanba and the staff of the Model Plant Research Facility at the National Institute for Basic Biology for plant growth support, and the Bioimaging Facility, NIBB Core Research Facilities for technical support.

Disclosures

The authors have no conflicts of interest to declare.

References

Aksam, E.B., Koek, A., Kiel, J.A., Jourdan, S., Veenhuis, M. and van der Klei, I.J. (2007) A peroxisomal lon protease and peroxisome degradation by autophagy play key roles in vitality of *Hansenula polymorpha* cells. *Autophagy* 3: 96–105.

Bartoszewska, M., Williams, C., Kikhney, A., Opalinski, L., van Roermund, C.W., de Boer, R. et al. (2012) Peroxisomal proteostasis involves a Lon family protein that functions as protease and chaperone. *J. Biol. Chem.* 287: 27380–27395.

Bayot, A., Gareil, M., Rogowska-Wrzesinska, A., Roepstorff, P., Friguet, B. and Bulteau, A.L. (2010) Identification of novel oxidized protein substrates and physiological partners of the mitochondrial ATP-dependent Lon-like protease Pim1. *J. Biol. Chem.* 285: 11445–11457.

Beevers, H. (1979) Microbodies in higher plants. *Annu. Rev. Plant Physiol.* 30: 159–193.

Bell, C.J. and Ecker, J.R. (1994) Assignment of 30 microsatellite loci to the linkage map of *Arabidopsis*. *Genomics* 19: 137–144.

Bissonnette, S.A., Rivera-Rivera, I., Sauer, R.T. and Baker, T.A. (2010) The IbpA and IbpB small heat-shock proteins are substrates of the AAA+ Lon protease. *Mol. Microbiol.* 75: 1539–1549.

Buchberger, A., Bukau, B. and Sommer, T. (2010) Protein quality control in the cytosol and the endoplasmic reticulum: brothers in arms. *Mol. Cell* 40: 238–252.

Clough, S.J. and Bent, A.F. (1998) Floral dip: a simplified method for *Agrobacterium*-mediated transformation of *Arabidopsis thaliana*. *Plant J.* 16: 735–743.

Collins, C.S., Kalish, J.E., Morrell, J.C., McCaffery, J.M. and Gould, S.J. (2000) The peroxisome biogenesis factors Pex4p, Pex22p, Pex1p, and Pex6p act in the terminal steps of peroxisomal matrix protein import. *Mol. Cell. Biol.* 20: 7516–7526.

Duman, R.E. and Löwe, J. (2010) Crystal structures of *Bacillus subtilis* Lon protease. *J. Mol. Biol.* 401: 653–670.

Farmer, L.M., Rinaldi, M.A., Young, P.G., Danan, C.H., Burkhart, S.E. and Bartel, B. (2013) Disrupting autophagy restores peroxisome function to an *Arabidopsis lon2* mutant and reveals a role for the LON2 protease in peroxisomal matrix protein degradation. *Plant Cell* 25: 4085–4100.

Footitt, S., Marquez, J., Schmuths, H., Baker, A., Theodoulou, F.L. and Holdsworth, M. (2006) Analysis of the role of *COMATOSE* and peroxisomal β-oxidation in the determination of germination potential in *Arabidopsis*. *J. Exp. Bot.* 57: 2805–2814.

Goldberg, A.L., Moerschell, R.P., Chung, C.H. and Maurizi, M.R. (1994) ATP-dependent protease La (lon) from *Escherichia coli*. *Methods Enzymol.* 244: 350–375.

Goto, S., Mano, S., Nakamori, C. and Nishimura, M. (2011) *Arabidopsis* ABERRANT PEROXISOME MORPHOLOGY9 is a peroxin that recruits the PEX1–PEX6 complex to peroxisomes. *Plant Cell* 23: 1573–1587.

Gur, E. and Sauer, R.T. (2009) Degrons in protein substrates program the speed and operating efficiency of the AAA+ Lon proteolytic machine. *Proc. Natl Acad. Sci. USA* 106: 18503–18508.

Gur, E., Vishkautzan, M. and Sauer, R.T. (2012) Protein unfolding and degradation by the AAA+ Lon protease. *Protein Sci.* 21: 268–278.

Hayashi, Y., Hayashi, M., Hayashi, H., Hara-Nishimura, I. and Nishimura, M. (2001) Direct interaction between glyoxysomes and lipid bodies in cotyledons of the *Arabidopsis thaliana ped1* mutant. *Protoplasma* 218: 83–94.

Iwata, J., Ezaki, J., Komatsu, M., Yokota, S., Ueno, T., Tanida, I. et al. (2006) Excess peroxisomes are degraded by autophagic machinery in mammals. *J. Biol. Chem.* 281: 4035–4041.

Kamada, T., Nito, K., Hayashi, H., Mano, S., Hayashi, M. and Nishimura, M. (2003) Functional differentiation of peroxisomes revealed by expression profiles of peroxisomal genes in *Arabidopsis thaliana*. *Plant Cell Physiol.* 44: 1275–1289.

Kanai, M., Hayashi, M. and Nishimura, M. (2010) A peroxisomal ABC transporter promotes seed germination by inducing pectin degradation under the control of *ABI5*. *Plant J.* 62: 936–947.

Kikuchi, M., Hatano, N., Yokota, S., Shimozawa, N., Imanaka, T. and Taniguchi, H. (2004) Proteomic analysis of rat liver peroxisome: presence of peroxisome-specific isozyme of Lon protease. *J. Biol. Chem.* 279: 421–428.

Konieczny, A. and Ausubel, F.M. (1993) A procedure for mapping *Arabidopsis* mutations using co-dominant ecotype-specific PCR-based markers. *Plant J.* 4: 403–410.

Leidhold, C. and Voos, W. (2007) Chaperones and proteases—guardians of protein integrity in eukaryotic organelles. *Ann. NY Acad. Sci.* 1113: 72–86.

Lingard, M.J. and Bartel, B. (2009) Arabidopsis LON2 is necessary for peroxisomal function and sustained matrix protein import. *Plant Physiol.* 151: 1354–1365.

Lingard, M.J., Monroe-Augustus, M. and Bartel, B. (2009) Peroxisome-associated matrix protein degradation in *Arabidopsis*. *Proc. Natl Acad. Sci. USA* 106: 4561–4566.

Lisenbee, C.S., Heinze, M. and Trelease, R.N. (2003) Peroxisomal ascorbate peroxidase resides within a subdomain of rough endoplasmic reticulum in wild-type Arabidopsis cells. *Plant Physiol.* 132: 870–882.

Mano, S., Nakamori, C., Fukao, Y., Araki, M., Matsuda, A., Kondo, M. et al. (2011) A defect of peroxisomal membrane protein 38 causes enlargement of peroxisomes. *Plant Cell Physiol.* 52: 2157–2172.

Mano, S., Nakamori, C., Hayashi, M., Kato, A., Kondo, M. and Nishimura, M. (2002) Distribution and characterization of peroxisomes in Arabidopsis by visualization with GFP: dynamic morphology and actin-dependent movement. *Plant Cell Physiol.* 43: 331–341.

Mano, S., Nakamori, C., Kondo, M., Hayashi, M. and Nishimura, M. (2004) An *Arabidopsis* dynamin-related protein, DRP3A, controls both peroxisomal and mitochondrial division. *Plant J.* 38: 487–498.

Mano, S., Nakamori, C., Nito, K., Kondo, M. and Nishimura, M. (2006) The Arabidopsis *pex12* and *pex13* mutants are defective in both PTS1- and PTS2-dependent protein transport to peroxisomes. *Plant J.* 47: 604–618.

Matsushima, R., Kondo, M., Nishimura, M. and Hara-Nishimura, I. (2003) A novel ER-derived compartment, the ER body, selectively accumulates a β-glucosidase with an ER-retention signal in *Arabidopsis*. *Plant J.* 33: 493–502.

Nakagawa, T., Kurose, T., Hino, T., Tanaka, K., Kawamukai, M., Niwa, Y. et al. (2007) Development of series of gateway binary vectors, pGWBs, for realizing efficient construction of fusion genes for plant transformation. *J. Biosci. Bioeng.* 104: 34–41.

Nakamura, S., Mano, S., Tanaka, Y., Ohnishi, M., Nakamori, C., Araki, M. et al. (2010) Gateway binary vectors with the bialaphos resistance gene, *bar*, as a selection marker for plant transformation. *Biosci. Biotechnol. Biochem.* 74: 1315–1319.

Nishimura, M., Hayashi, M., Kato, A., Yamaguchi, K. and Mano, S. (1996) Functional transformation of microbodies in higher plant cells. *Cell Struct. Funct.* 21: 387–393.

Nishimura, M., Takeuchi, Y., De Bellis, L. and Hara-Nishimura, I. (1993) Leaf peroxisomes are directly transformed to glyoxysomes during senescence of pumpkin cotyledons. *Protoplasma* 175: 131–137.

Nishimura, M., Yamaguchi, J., Mori, H., Akazawa, T. and Yokota, S. (1986) Immunocytochemical analysis shows that glyoxysomes are directly transformed to leaf peroxisomes during greening of pumpkin cotyledons. *Plant Physiol.* 81: 313–316.

Omi, S., Nakata, R., Okamura-Ikeda, K., Konishi, H. and Taniguchi, H. (2008) Contribution of peroxisome-specific isoform of Lon protease in sorting PTS1 proteins to peroxisomes. *J. Biochem.* 143: 649–660.

Ostersetzer, O., Kato, Y., Adam, Z. and Sakamoto, W. (2007) Multiple intracellular locations of Lon protease in Arabidopsis: evidence for the localization of AtLon4 to chloroplasts. *Plant Cell Physiol.* 48: 881–885.

Rep, M., van Dijl, J.M., Suda, K., Schatz, G., Grivell, L.A. and Suzuki, C.K. (1996) Promotion of mitochondrial membrane complex assembly by a proteolytically inactive yeast Lon. *Science* 274: 103–106.

Reumann, S., Quan, S., Aung, K., Yang, P.F., Manandhar-Shrestha, K., Holbrook, D. et al. (2009) In-depth proteome analysis of Arabidopsis leaf peroxisomes combined with in vivo subcellular targeting verification indicates novel metabolic and regulatory functions of peroxisomes. *Plant Physiol.* 150: 125–143.

Rigas, S., Daras, G., Laxa, M., Marathias, N., Fasseas, C., Sweetlove, L.J. et al. (2009) Role of Lon1 protease in post-germinative growth and maintenance of mitochondrial function in *Arabidopsis thaliana*. *New Phytol.* 181: 588–600.

Rigas, S., Daras, G., Tsitsekian, D. and Hatzopoulos, P. (2012) The multifaceted role of Lon proteolysis in seedling establishment and maintenance of plant organelle function: living from protein destruction. *Physiol. Plant.* 145: 215–223.

Rotanova, T.V., Botos, I., Melnikov, E.E., Rasulova, F., Gustchina, A., Maurizi, M.R. et al. (2006) Slicing a protease: structural features of the ATP-dependent Lon proteases gleaned from investigations of isolated domains. *Protein Sci.* 15: 1815–1828.

Sakai, Y., Oku, M., van der Klei, I.J. and Kiel, J.A. (2006) Pexophagy: autophagic degradation of peroxisomes. *Biochim. Biophys. Acta* 1763: 1767–1775.

Sauer, R.T., Bolon, D.N., Burton, B.M., Burton, R.E., Flynn, J.M., Grant, R.A. et al. (2004) Sculpting the proteome with AAA(+) proteases and disassembly machines. *Cell* 119: 9–18.

Schluter, A., Fourcade, S., Ripp, R., Mandel, J.L., Poch, O. and Pujol, A. (2006) The evolutionary origin of peroxisomes: an ER–peroxisome connection. *Mol. Biol. Evol.* 23: 838–845.

Shibata, M., Oikawa, K., Yoshimoto, K., Kondo, M., Mano, S., Yamada, K. et al. (2013) Highly oxidized peroxisomes are selectively degraded via autophagy in *Arabidopsis thaliana*. *Plant Cell* 25: 4967–4983.

Solheim, C., Li, L., Hatzopoulos, P. and Millar, A.H. (2012) Loss of Lon1 in Arabidopsis changes the mitochondrial proteome leading to altered metabolite profiles and growth retardation without an accumulation of oxidative damage. *Plant Physiol.* 160: 1187–1203.

Stahlberg, H., Kutejova, E., Suda, K., Wolpensinger, B., Lustig, A., Schatz, G. et al. (1999) Mitochondrial Lon of *Saccharomyces cerevisiae* is a ring-shaped protease with seven flexible subunits. *Proc. Natl Acad. Sci. USA* 96: 6787–6790.

Titus, D.E. and Becker, W.M. (1985) Investigation of the glyoxysome–peroxisome transition in germinating cucumber cotyledons using double-label immunoelectron microscopy. *J. Cell Biol.* 101: 1288–1299.

Toyota, M., Matsuda, K., Kakutani, T., Terao Morita, M. and Tasaka, M. (2011) Developmental changes in crossover frequency in Arabidopsis. *Plant J.* 65: 589–599.

Van Melderen, L. and Gottesman, S. (1999) Substrate sequestration by a proteolytically inactive Lon mutant. *Proc. Natl Acad. Sci. USA* 96: 6064–6071.

Wagner, I., Arlt, H., van Dyck, L., Langer, T. and Neupert, W. (1994) Molecular chaperones cooperate with PIM1 protease in the degradation of misfolded proteins in mitochondria. *EMBO J.* 13: 5135–5145.

Yamada, K., Nagano, A.J., Nishina, M., Hara-Nishimura, I. and Nishimura, M. (2008) NAI2 is an endoplasmic reticulum body component that enables ER body formation in *Arabidopsis thaliana*. *Plant Cell* 20: 2529–2540.

Yokota, S., Haraguchi, C.M. and Oda, T. (2008) Induction of peroxisomal Lon protease in rat liver after di-(2-ethylhexyl)phthalate treatment. *Histochem. Cell Biol.* 129: 73–83.

Yoshimoto, K., Hanaoka, H., Sato, S., Kato, T., Tabata, S., Noda, T. et al. (2004) Processing of ATG8s, ubiquitin-like proteins, and their deconjugation by ATG4s are essential for plant autophagy. *Plant Cell* 16: 2967–2983.

Youle, R.J. and van der Bliek, A.M. (2012) Mitochondrial fission, fusion, and stress. *Science* 337: 1062–1065.